Recent results of baryon EM form factors at BESIII

Yadi Wang[1,*]
(on behalf of BESIII Collaboration)

[1]North China Electric Power University, Beinong Road No. 2, Beijing, China

Abstract. Precise experimental measurements of the baryon form factors are a test-bed for understanding the baryon's properties and dynamical behavior emerge from QCD. With high statistics, the cross section of $e^+e^- \to p\bar{p}$ and $e^+e^- \to n\bar{n}$ are both measured with the highest precision in a wide q^2 range. The oscillation behavior on the proton and neutron effective form factor is updated with SND result. With the ISR technique, the form factor measurement can reach as low as the mass threshold of $p\bar{p}$ or $n\bar{n}$. Analyticity of nucleon form factors is discussed. Moreover, new results about the hyperon (Λ, Λ_c, Σ, Ω, Δ) form factors are presented in this talk. Some similar behaviors appear on the hyperon form factors which will help to understand the internal structure or interactions inside of the baryon. The complete determination of EMFFs of Λ and Σ has been carried on and provides a new insight of EMFFs in time-like region.

1 Introduction

The discovery that the majority of the nucleon spin is not carried by the valence quarks [1], as naively expected, is a proof of how complicated the nucleon structure is. At low q^2, the perturbative QCD is not suitable to make a clear prediction, the inner structure of baryons must be studied by experiment. The structure of the proton has been extensively studied with great success exploiting the lepton-hadron scattering in space-like (SL) region. Alternatively, the e^+e^- collider contributes to the baryon structure by studying the fragmentation functions and electromagnetic (EM) form factors (FF) in time-like (TL) region.

The EMFFs describe charge and magnetization distributions of non-point-like particles, and help to discover fundamental properties of the baryons. They are crucial testing ground for various models. The dispersion theoretical analysis provides a coherent framework for the joint interpretation of SL and TL EMFFs over the entire physical range of q^2 although it needs data also in the unphysical region. For spin$-\frac{1}{2}$ baryons, assuming one-phone exchange, first suggested by N. Cabibbo and R. Gatto in 1961 [2], the Born cross section of baryon pair production is expressed as Eq. 1:

$$\frac{d\sigma}{d\cos\theta} = \frac{\pi\alpha^2\beta C}{2q^2}[|G_M|^2(1+\cos^2\theta) + \frac{1}{\tau}|G_E|^2\sin^2\theta], \tag{1}$$

where $\tau = \frac{4m^2}{q^2}$, $C = \frac{\pi\alpha}{\beta}\frac{1}{1-exp(-\frac{\pi\alpha}{\beta})}$ is the Coulomb factor, and m is the mass of baryon. Here, α is the EM fine structure constant, $\beta = \sqrt{1-4m_B^2c^4/s}$ is the baryon velocity. At threshold,

*e-mail: wangyadi@ncepu.edu.cn

© The Authors, published by EDP Sciences. This is an open access article distributed under the terms of the Creative Commons Attribution License 4.0 (https://creativecommons.org/licenses/by/4.0/).

it is required that $G_E = G_M = G$ because the final particle momentum is zero and the final hadrons must be symmetrically distributed around collision axis. In other word, only S-wave contributes, and no D-wave at threshold.

The Coulomb factor C is a correction to the one-photon exchange and describes the EM interaction between the outgoing baryon pairs. For neutral baryons this factor should be $C = 1$. Hence, a vanishing cross section should be expected close to the threshold, because of the phase space β factor. For charged baryons, usually C is assumed to have the value for pointlike charged fermions $C = \epsilon R$ [4], where $\epsilon = \pi\alpha/\beta$ is an enhancement factor, resulting in a nonzero cross section at threshold, because of the cancellation between the two β factors. $R = \sqrt{1-\beta^2}/(1 - e^{-\pi\alpha\sqrt{1-\beta^2}/\beta})$ is the so-called Sommerfeld resummation factor [5].

Space-like EMFFs are real functions of q^2, whereas the time-like ones are complex. The electric and the magnetic form factor of a spin 1/2 baryon have a relative phase $\Delta\Phi$ [3] ($\frac{G_E}{G_M} = e^{i\Delta\Phi}|\frac{G_E}{G_M}|$), reflecting fluctuations of the γ^* into *e.g.* a $\pi\pi$ intermediate state. The non-zero phase manifests a polarization in the final state, even if the colliding beams are unpolarized, which is proportional to $\sin\Delta\Phi$:

$$P_y = \frac{\sqrt{1-\eta^2}\sin\theta\cos\theta}{1+\eta\cos^2\theta}\sin(\Delta\Phi), \tag{2}$$

where $\eta = (\tau - R_{EM}^2)/(\tau + R_{EM}^2)$, $R_{EM} = |G_E/G_M|$.

In 1972, the first experiment on the reaction in $e^+e^- \to p\bar{p}$ was performed at ADONE at a center-of-mass (c.m.s.) energy of 2.1 GeV. Using spark-chamber counter, an integrated luminosity of 0.19 pb^{-1} of data was collected, and finally 25 signal events had been selected. The cross section of $e^+e^- \to p\bar{p}$ is measured as 0.73 ± 0.18 nb at 2.1 GeV. Later, energy scan method and initial state radiation (ISR) method are both developed and used for the Born cross section measurement of baryon pair productions from e^+e^- annihilation. The energy scan method gives a well-defined c.m.s. energy with low background, and it has a very good energy resolution, but discrete values which leave gaps between the energy points. Experiments of CLEO-c, CMD-3, SND do the measurements with energy scan method, while the ISR method collects data at a fixed c.m.s. energy, thus the momentum transferred q^2 is from $p\bar{p}$ threshold to $\sqrt{s}$, and the systematic uncertainty is controlled in a coherent way. At the same time, the ISR method needs large luminosity, and the background is higher. Experiments, such as BaBar and BELLE can do the measurements with ISR method. Out of them, BESIII is the only experiment that can handle both techniques. The BESIII spectrometer which is located at BEPCII in Beijing is described in Ref. [6], and will not be discussed in this paper.

2 Proton EMFFs

The early results for the cross section of $e^+e^- \to p\bar{p}$ were addressed by DM1 [7], DM2 [8] and FENICE [9] before 21 century, with large errors and in a limited narrow energy region. The G_E/G_M was measured with very poor precision with PS170 experiment [10]. From 2005 to 2015, results from BaBar experiment dominated [11], with better precision on the Born cross section via ISR method, as well as the G_E/G_M ratio, but with obviously different trend. From BaBar, the cross section at threshold is different from zero. There is a sharp rise of the cross section up to about 850 pb followed by a plateau up to about 200 MeV above threshold. The cross sections at threshold and at the plateau are, within the errors, surprisingly close to the expected value for the pointlike $p\bar{p}$ production. To obtain the aforementioned plateau, it is natural to consider the pointlike Coulomb factor, which increases very quickly at the threshold causing a non-zero cross section, and decreases quickly a few MeV above threshold. In order

to explain such a FF behavior, various FSI[12] models, related to the strong nucleon-nucleon cross section at very low c.m.s. energies, have been put forward.

In 2019, CMD3 reanalyzed the new dataset in $p\bar{p}$ channel combined with $3(\pi^+\pi^-)$ and $K^+K^-\pi^+\pi^-$ channels [13], and confirm the step behavior observed by FENICE, CMD-3, BaBar, and BESIII. The step behavior from three channels is described with an exponentially saturated function for a very fast variation of the cross section. Explained by final state interaction (FSI) theory, the total hadronic cross section is strongly affected by virtual production and annihilation of the $N\bar{N}$ pairs. A naive expectation suggests that the effect could be proportional to the probability of $p\bar{p}$ annihilation into the studied final state. However, out of expectation, no structure has been observed in the $e^+e^- \to 2(\pi^+\pi^-)$ cross section.

From 2020 to 2022, BESIII published its results with best precision via energy scan method and ISR method based on its largest datasets in the world. For the first time, the $|G_E/G_M|$ and $|G_M|$ are determined with high accuracy, and comparable to data in SL region [14]. The $|G_E|$ is measured also for the first time. Data from both methods give consistent results on the effective form factor $|G_{eff}|$ and a damped oscillation behavior on the $|G_{eff}|$ distribution after subtracting the dipole function [15–17], shown in Fig. 1.

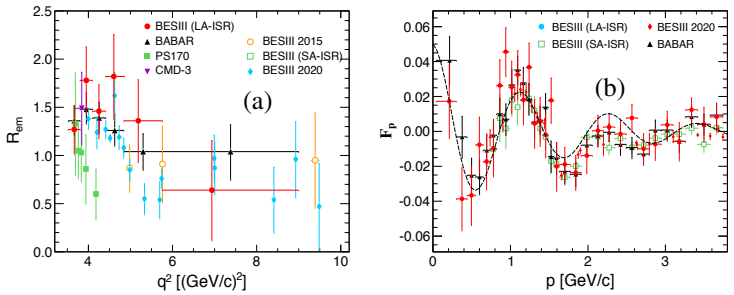

Figure 1. (a) The ratio between form factors $R = |G_M|/|G_E|$ compared with other experimental results. (b) The residual effective form factor F_p.

2.1 Neutron EMFFs

The first measurements of the neutron TL EMFFs were reported in the 1990s by FENICE [18] and the DM2 [19] experiments with very poor statistics, and no data on the $|G_E/G_M|$ ratio. The SND experiment reported its result [20] in 2014 for the cross section of $e^+e^- \to n\bar{n}$ and indicated a plateau near the threshold, but the precision is not good enough to confirm.

In 2021, based on 647.9 pb^{-1} scan data from 2.0 to 3.08 GeV, BESIII published the unprecedented results on the Born cross section and the effective form factors $|G|$ of the neutron [21]. With the results on the Born cross section of $e^+e^- \to p\bar{p}$ from BESIII with the same dataset, the ratio $R_{np} = \sigma_B^{n\bar{n}}/\sigma_B^{p\bar{p}}$ is less than 1 for all energy points, shown in Fig. 2 (a), and this conflicts with results from FENICE. This result shows the photon-proton interaction is stronger than the corresponding photon-neutron interaction, as expected by most theoretical predictions, and clarifies the photon–nucleon interaction puzzle that has persisted for over 20 years.

Very interestingly, the effective form factor of neutron shows also an oscillating behavior. The residual $G_{osc}(q^2) = |G| - G_D$, $G_D = A_n/(1 - \frac{q^2}{0.71(GeV^2)})^2$ is shown in in Fig. 2 (b). The parameter $A_n = 4.87 \pm 0.09$ is calculated with BaBar result. The periodic structure $G_{osc}(q^2)$ is parameterized similarly to $e^+e^- \to p\bar{p}$, but with a relative phase of $\Delta D = (125 \pm 12)^\circ$.

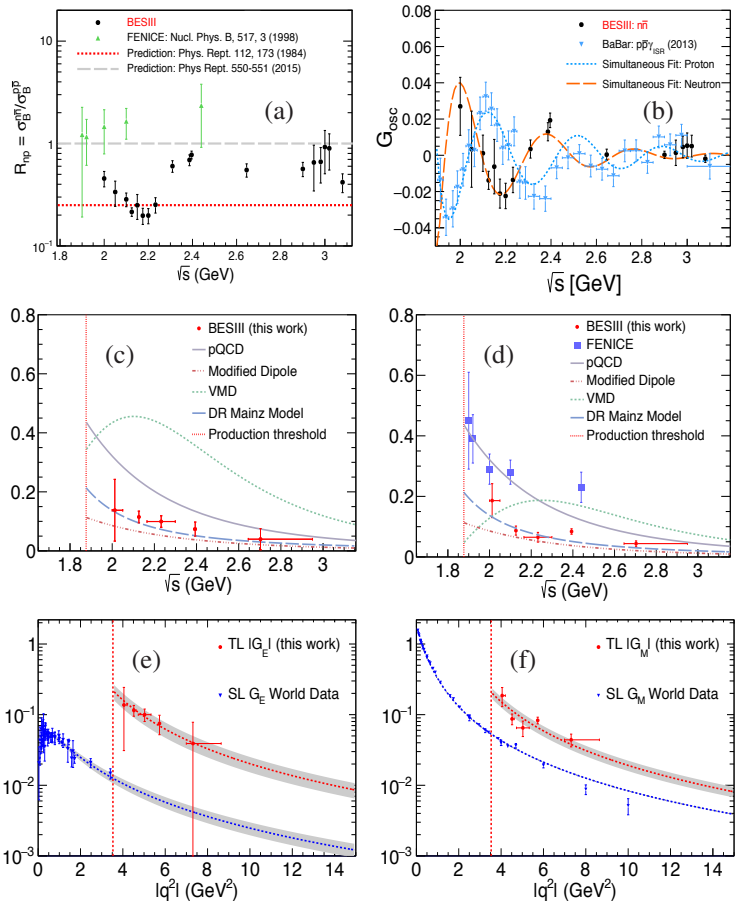

Figure 2. (a) The ratio (R_{np}) between Born cross section of $e^+e^- \to p\bar{p}$ and $e^+e^- \to n\bar{n}$. (b) The residual effective form factor $G_{osc}(q^2)$ of neutron compared with other experimental results. (c) and (d) are results for the separated form factors of the neutron: (c) for electric and (d) for magnetic form factors compared with different model predictions. (e) is electric and (f) is magnetic form factors as a function of $|q^2|$ from BESIII [23] shown together with results from the world data of SL ones.

Last year, SND experiment published the results on $e^+e^- \to n\bar{n}$ at c.m.s. energies from 1.894 to 2 GeV [22]. The value of the Born cross section below 2 GeV is about 0.4 nb lower than BESIII and previous results. The effective neutron form factor is also calculated and analyzed together with BESIII and BaBar data. The SND result strongly contradicts the prediction that was extracted from a simultaneous fit to the BaBar proton and BESIII neutron data.

BESIII published the newest results on the neutron EMFFs recently [23]. The independent results on $|G_E|$ and $|G_M|$ are given, and compared with different theoretical models, shown in Fig. 2 (c) and (d). As stated in the Phragmen-Lindelof (P-L) theorem, EMFFs in the TL region can be extended to any direction of the q^2 complex plane. As a result, the numerical values of EMFFs should approach each other for $|q^2| \to \infty$. In other words, the ratio $R_{E,M} = |G^{TL}_{E,M}(q^2)/G^{SL}_{E,M}(-q^2)|$ goes to 1 when $q^2 \to \infty$. While, our result shows

$R_E = 5.18 \pm 1.18$ for $|G_E|$ and $R_M = 1.72 \pm 0.14$ for $|G_M|$. All these interesting results from proton and neutron will provide theorists much information on the nucleon structure and QCD.

3 Hyperon EMFFs

The EMFFs of hyperons provide powerful complementary information of nucleon. A systematic comparison of octet baryons sheds light on what extent SU(3) flavor symmetry is broken. The importance of hyperon structure was pointed out as early as 1960, but has not been subjected to rigorous experimental studies until recent decades. The main reason is that SL TMFFs of hyperons are not straightforward to access experimentally since their finite lifetime makes them unsuitable as beams or targets. Instead, the EMFFs can be accessed from $e^+e^- \to \gamma^* \to Y\bar{Y}$, where Y denotes the hyperon.

Before 2000, there were very few results for the hyperon EMFFs from DM2 and only below 2.4 GeV with poor precision. From 2005 to 2015, BaBar measured the hyperon (Λ, Σ^0 and $\Lambda\Sigma^0$) EMFFs, via ISR method. Still the precision is not good. From 2015, a series of measurement on hyperon EMFFs have been performed at BESIII with unprecedented large statistics. Here, we report some of them.

3.1 Cross section measurement on $e^+e^- \to \Lambda\bar{\Lambda}$, $\Lambda_c\bar{\Lambda}_c$, $\Sigma\bar{\Sigma}$, $\Omega\bar{\Omega}$, and $\Delta\bar{\Delta}$

The cross section of $e^+e^- \to \Lambda\bar{\Lambda}$ was measured with 11.9 fb^{-1} data collected from 3.772 to 4.258 GeV by ISR method. The non-zero cross section is consistent with our previous measurement and those from BaBar and DM2 [24]. We also observed a very sharp peak just above the threshold, shown in Fig. 3 (a), which arose a lot of theoretical discussions.

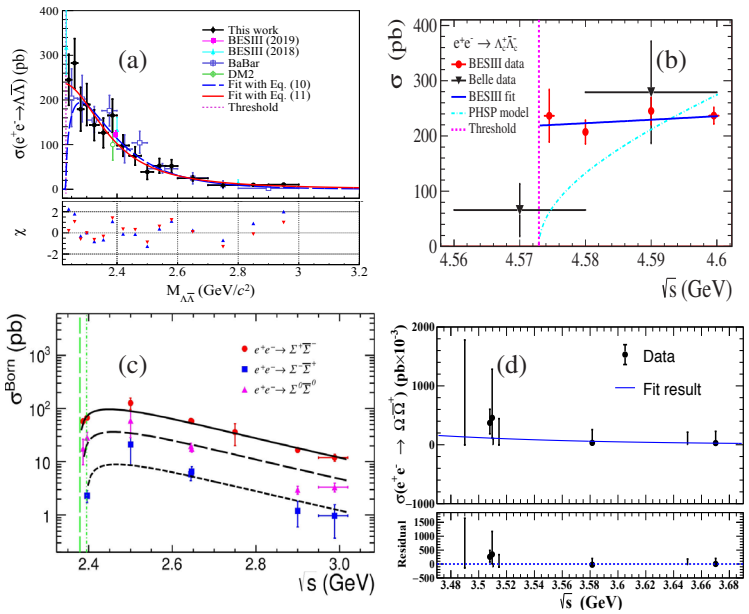

Figure 3. The cross section of $e^+e^- \to$ (a) $\Lambda\bar{\Lambda}$; (b) $\Lambda_c\bar{\Lambda}_c$; (c) $\Sigma\bar{\Sigma}$; (d) $\Omega\bar{\Omega}$.

A measurement based on the XYZ dataset is performed for the cross section measurement of $e^+e^- \to \Lambda_c\bar{\Lambda}_c$. Similar with $e^+e^- \to p\bar{p}$, its lineshape indicates that there is indeed a plateau following the threshold, shown in Fig. 3 (b). The cross section of the first energy point which is only 1.5 MeV above threshold is $236 \pm 11 \pm 46$ pb which is far from zero. The $|G_E/G_M|$ is measured at two energy points, and the value is consistent with unity.

Precision measurements of $e^+e^- \to \Sigma\bar{\Sigma}$ with a data sample of about 330 pb^{-1} collected at BESIII with c.m.s energies between 2.3864 and 3.0200 GeV are done. Unlike $e^+e^- \to p\bar{p}$ or $\Lambda\bar{\Lambda}$, no significant threshold effects are observed in these processes [25]. Instead, a perturbative-QCD driven function can describe the cross section lineshapes well. An asymmetry in results is observed for the isospin triplet, with the Σ^+ results lying above the Σ^0 results which in turn are higher than the Σ^- results, shown in Fig. 3 (c). This behavior confirms the hypothesis that the effective FF is proportional to $\sum_q Q_q^2$ with $q = u, d, s$ quarks. Moreover, the effective form factor of the Σ^0 is compared with that of the Λ to test the diquark correlation model. Belle published their $\Sigma^+\bar{\Sigma}^-$ cross section result with ISR method [26], which fill the gap of $2.4 \sim 2.5$ GeV and $2.5 \sim 2.6$ GeV. And their result is consistent with our results within uncertainty.

With the same scan datasets, the Born cross sections of $e^+e^- \to \Omega\bar{\Omega}$ and $\Delta\bar{\Delta}$ are searched for. No significant signal is observed for either channel. Thus, upper limit of cross section as well as the effective FF is given, as shown in Fig. 3 (d). They are consistent with the pQCD driven prediction.

3.2 Complete measurement of hyperon EMFFs

The relative phase $\Delta\Phi$ of $G_E(q^2)$ and $G_M(q^2)$ governs the vector polarization and tensor polarization (*i.e.* spin correlations) of the produced hyperon-antihyperon pair [27]. If the beams are unpolarized, a vector polarization of the final hyperons is only allowed in the direction normal to the plane spanned by the incoming beam and the outgoing hyperon. A complete decomposition of the complex G_E and G_M requires a multidimensional analysis of the reaction and the subsequent baryon decays. The joint decay distribution of $e^+e^- \to \Lambda\bar{\Lambda}(\Lambda \to p\pi^-, \bar{\Lambda} \to \bar{p}\pi^+)$ was derived in terms of $\Delta\Phi$ and a series of angular distribution parameters, see Ref. [27].

The Λ transverse polarization P_y is given by Eq. 2. The plot of $\alpha_\Lambda P_y$ versus scattering angle $\cos\theta$ of Λ extracted from data is shown in Fig. 4 (a), and the data points are fitted with theoretical predictions in Ref. [27]. The $|G_E/G_M|$ is determined to be $0.96 \pm 0.14_{stat.} \pm 0.02_{syst.}$, and $\Delta\Phi = (37 \pm 12_{stat.} \pm 6_{syst.})^\circ$. This result confirms the complex form of EMFFs in TL region. Later on, various models try to use our measurement for theoretical discussion. More measurements of the relative phase in a wide q^2 range are needed since they are crucial to enhance the predictive power of various models and test the aymptotic behavior in TL and SL regions.

As a preliminary result shown here, the complete measurement of Σ^+ EMFFs is performed very recently by a similar joint angular distribution as Λ. The polarization is observed at 2.396, 2.644, and 2.90 GeV with a significance of 2.2σ, 3.6σ and 4.1σ. The relative phase $\Delta\Phi$ and $|G_E/G_M|$ ratio are compared with a $Y\bar{Y}$ model [28], but have a different tendency in $\Delta\Phi$, shown in Fig. 4 (b). In addition, the $\Delta\Phi$ distribution indicates that there are integer multiples of π radians, from threshold to the cross point. The $\Delta\Phi$ increases with q^2, which indicates that the asymptotic threshold has not yet been reached. Thus, more experimental results are needed to understand these questions more deeply.

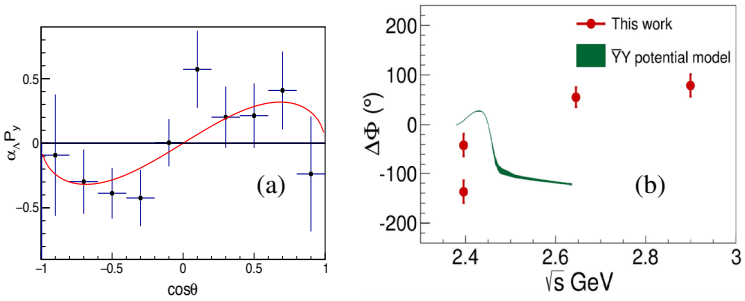

Figure 4. (a) The product of α_Λ and Λ polarization P_y as a function of the scattering angle. (b) Results for the relative phase $\Delta\Phi$ of $\Sigma\bar{\Sigma}$, and the green band represent the theoretical prediction from a $Y\bar{Y}$ potential model [28].

4 Summary

In summary, based on energy scan method and ISR method, fruitful and interesting physics results for the baryon EMFFs from e^+e^- collider are obtained. The conventional parameterization of EMFFs is facing big challenge from the experimental observations. The baryonic threshold effect, the oscillation in reduced FFs, the behavior of G_E/G_M ratio and other problems are all urgent to be understood both from experiments and theories. The relative phase of EMFFs gives rise to polarization of final baryons, and this will play an important role in distinguishing various theoretical models. Last but not least, the asymptotic behavior of baryon EMFFs has been tested in serval baryonic pair decays, but the asymptotic threshold has not yet been reached. We are expecting to get more and more physics results on the baryon EMFFs in the future.

References

[1] J. Ashman *et al.*, Phys. Lett. B. **206**, 206 (1988)
[2] N. Cabibbo and R. Gatto, Physical Review **124**, 5 (1961)
[3] A. Z. Dubnickova, S. Dubnicka, and M. P. Rekalo, Nuovo Cim. A, **109**, 241 (1996)
[4] A. D. Sakharov, Sov. Phys. Usp **34**, 375 (1991)
[5] A. Sommerfeld, Ann. Phys. **403**, 257 (1931)
[6] M. Ablikim (BESIII Collaboration), Nucl. Ins. and Meth. in Phys. Res. A **614**, 345 (2010)
[7] B. Delcourt *et al.* (DM1 Collaboration), Phys. Lett. B **86**, 395 (1979)
[8] D. Bisello *et al.* (DM2 Collaboration), Nucl. Phys. B **224**, 379 (1983); Z. Phys. C **48**, 23 (1990)
[9] A. Antonelli *et al.* (FENICE Collaboration), Nucl. Phys. B **517**, 3 (1998)
[10] G. Bardin *et al.* (PS170 Collaboration), Nucl. Phys. B **411**, 3 (1994)
[11] J. P. Lees *et al.* (BaBar Collaboration), Phys. Rev. D **73**, 012005 (2006); **87**, 092005 (2013); **88**, 072009 (2013)
[12] J. Haidenbauer, X.W. Kanga, U.G. Meissner, Nucl. Phys. A **929**, 102 (2014)
[13] R.R. Akhmetshin *et al.*, Phys. Lett. B **794**, 64 (2019)
[14] M. Ablikim (BESIII Collaboration), Phys. Rev. Lett. **124**, 042001 (2020)

[15] A. Bianconi and E. Tomasi Gustafsson, Phys. Rev. Lett. **114**, 232301 (2015)
[16] M. Ablikim (BESIII Collaboration), Phys. Rev. D **99**, 092002 (2019)
[17] M. Ablikim (BESIII Collaboration), Phys. Lett. B **817**, 136328 (2021)
[18] A. Antonelli *et al.* (FENICE Collaboration), Nucl. Phys. B **517**, 3 (1998)
[19] D. Bisello *et al.* (DM2 Collaboration), Z. Phys. C **48**, 23 (1990)
[20] M. N. Achasov *et al.* (SND Collaboration), Phys. Rev. D **90**, 112007 (2014)
[21] M. Ablikim (BESIII Collaboration), Nature Physics **17**, 1200 (2021)
[22] M. N. Achasov *et al.* (SND Collaboration), Eur. Phys. J. C **82**, 761 (2022)
[23] M. Ablikim (BESIII Collaboration), Phys. Rev. Lett. **130**, 151905 (2023)
[24] M. Ablikim (BESIII Collaboration), Phys. Rev. D **107**, 072005 (2023)
[25] M. Ablikim (BESIII Collaboration), Phys. Lett. B **814**, 136110 (2021); Phys. Lett. B **831**, 137187 (2022)
[26] G. Gong *et al.* (Belle Collaboration), Phys. Rev. D **107**, 072008 (2023)
[27] G. Faldt, Phys. Rev. D **97**, 053002 (2018)
[28] J. Haidenbauer, U. G. Meißner, and L. Y. Dai, Phys. Rev. D **103**, 014028 (2021)